

Interference Coordination: Random Clustering and Adaptive Limited Feedback

Salam Akoum and Robert W. Heath, Jr.

Abstract—Interference coordination improves data rates and reduces outages in cellular networks. Accurately evaluating the gains of coordination, however, is contingent upon using a network topology that models realistic cellular deployments. In this paper, we model the base stations locations as a Poisson point process to provide a better analytical assessment of the performance of coordination. Since interference coordination is only feasible within clusters of limited size, we consider a random clustering process where cluster stations are located according to a random point process and groups of base stations associated with the same cluster coordinate. We assume channel knowledge is exchanged among coordinating base stations, and we analyze the performance of interference coordination when channel knowledge at the transmitters is either perfect or acquired through limited feedback. We apply intercell interference nulling (ICIN) to coordinate interference inside the clusters. The feasibility of ICIN depends on the number of antennas at the base stations. Using tools from stochastic geometry, we derive the probability of coverage and the average rate for a typical mobile user. We show that the average cluster size can be optimized as a function of the number of antennas to maximize the gains of ICIN. To minimize the mean loss in rate due to limited feedback, we propose an adaptive feedback allocation strategy at the mobile users. We show that adapting the bit allocation as a function of the signals' strength increases the achievable rate with limited feedback, compared to equal bit partitioning. Finally, we illustrate how this analysis can help solve network design problems such as identifying regions where coordination provides gains based on average cluster size, number of antennas, and number of feedback bits.

I. INTRODUCTION

Coordination can mitigate interference and increase data rates in cellular systems [1]. Complete coordination between all the base stations in the network, however, is not feasible [2], [3]. For inter-base station overhead to be affordable, only groups of base stations coordinate, forming coordination clusters [2], [4], [5]. To quantify the gains from coordination, an accurate model of the network topology and the relative locations of the mobile users and the base stations needs to be considered [4]. Much prior analytical work on interference coordination used oversimplified network models and reported coordination gains that did not materialize in practical cellular deployment scenarios [6]. This paper addresses this issue by considering a point process model for deployment and clustering of base stations.

Most of the literature on interference coordination [1], [4], [5], [7]–[14] considered fixed cellular network architectures such as the Wyner model or the hexagonal grid. The Wyner

model is used to derive information theoretic bounds on the performance of multicell cooperation [1], [4], [7]; it does not account for the random locations of the users inside the cells. Hexagonal grid models, although reasonably successful in studying cellular networks, generally rely on extensive Monte Carlo simulations to gain insight into effective system design parameters [2], [15]. Using random models for the base stations locations yields, under fairly simple assumptions, analytical characterizations of outage and capacity, and provides a good approximation for the performance of actual base stations deployment [16].

We consider randomly deployed base stations. To form coordinating base station clusters, we propose a random clustering model, in which cluster stations are randomly deployed in the plane, and base stations connect to their geographically closest cluster station. The random clustering model builds on the analytical appeal of the random network deployment. It mirrors the connection of base transceiver stations to their base station controllers in current cellular systems [17]. A similar hierarchical structure was used in [18] to model traffic and requests for communication in wired telecommunication networks. A regular lattice clustering model of randomly deployed base stations was considered in [19] to derive the asymptotic outage performance of interference coordination as a function of the location of the user inside the fixed grid and the scattering model.

To achieve coordination gains, coordinating base stations exchange channel state information (CSI) on the backhaul. Each base station designs its beamforming vector to transmit exclusively to the users in its own cell, while exchanging CSI of the served users with the cooperating base stations. Examples of interference coordination strategies in the literature [8]–[10], [12], [13] include iterative strategies such as MMSE estimation beamforming [10] and non-iterative strategies such as intercell interference nulling (ICIN) [9], [12], [13]. ICIN is a cooperative beamforming strategy where each base station transmits in the null space of its interference channels.

The gains from coordination depend on the quality of CSI available to the base stations. In frequency division duplex systems, the CSI of the estimated channels at the mobile users can be made available at the base stations through feedback. The feedback channel possesses finite bandwidth and thus limited feedback techniques [20] are employed. Most of the literature on multicell coordination [5], [11], [14] assumes full CSI at the transmitters, neglecting the performance loss due to quantization. For ICIN with limited feedback, each mobile user quantizes and feeds back the CSI of the desired and interfering channels. This is in contrast with single-cell limited feedback, where only the CSI of the desired channel is fed

S. Akoum and R. Heath are with The University of Texas at Austin, 2501 speedway stop C0806, Austin, TX 78712 USA (e-mail: salam.akoum, rheath@mail.utexas.edu). This work was funded in part by Huawei Technologies.

back [21]. Dividing the feedback budget among the desired and interfering channels has been proposed as a reasonable approach for ICIN with limited feedback [13], [22]. The allocation of bits to channels at the receiver can be done equally or adaptively, taking into account the location of the user and the strength of the channel being quantized [13].

In this paper, we analyze the performance gains of interference coordination in a clustered network model where the base station locations are distributed as an independent homogeneous Poisson point process (PPP) and the clustering of the base stations is done through overlaying another independent homogeneous PPP. Base stations belonging to the same cluster coordinate via ICIN. We account for the feasibility of ICIN given the number of interferers in each cluster and the number of antennas at each base station. We distinguish between two cases, first assuming that ICIN is always feasible, and later considering a preset number of antennas at each base station and only applying ICIN when feasible. Single-cell beamforming is applied otherwise. Using tools from stochastic geometry, we derive a bound on the coverage and average rate performance of the proposed clustered coordination model for both cases. For the case of limited feedback CSI, we derive a bound on the mean loss in rate. We assume random vector quantization (RVQ) at the mobile users for analytical reasons. To minimize the mean loss in rate due to quantization, we consider an adaptive bit allocation algorithm and we derive closed form expressions to determine the number of bits to allocate to each channel based on its strength.

The contributions of the paper are summarized as follows.

- We propose a random hierarchical clustering model based on point process deployment of cluster stations and base stations. We assume that the base stations connect to their geographically closed cluster stations to form coordination clusters.
- We derive bounds on the coverage and average rate performance of ICIN, for the proposed clustered model, as a function of the number of interferers inside each cluster, the number of antennas at each base station, and the average cluster size.
- We analyze the feasibility of ICIN taking into account the random number of interferers inside each cluster and the number of antennas at the base stations. We propose a thresholding policy where ICIN is applied only when feasible, and single-cell beamforming is applied otherwise. We derive bounds on the probability of coverage and average rate performance of the thresholding policy. We show that there is an optimal cluster size to achieve maximum coordination gains.
- We derive an upper bound on the mean loss in rate due to limited feedback using ICIN. The bound is a function of the number of feedback bits allocated to each channel, the number of interferers, and the relative channel strengths at the mobile user. We derive closed form expressions for allocating the feedback bits to the desired and interfering channels, as a function of their relative strengths at the mobile user, and taking into account the relative strength of the inter-cluster and intra-cluster interference.

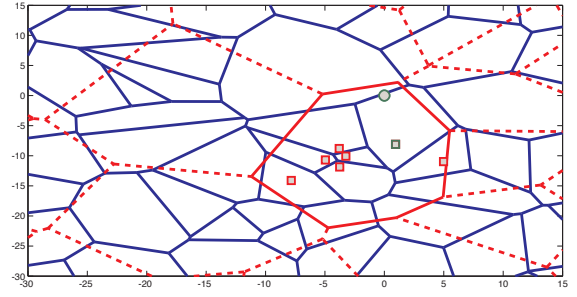


Fig. 1. The hierarchical cellular model considered. The Voronoi tessellation of the plane formed by the cells of Π_b is shown in blue. The Voronoi tessellation formed by Π_c is shown in red. The typical mobile user is shown in a green circle. The cooperating base stations for the cluster of interest are shown in rectangles.

Throughout the paper, we use the following notation, \mathbf{a} is a column vector, \mathbf{A} is a matrix, a is a scalar. \mathbf{A}^* denotes the conjugate transpose and \mathbf{A}^{-1} the matrix inverse. The left pseudo-inverse of \mathbf{A} with linearly independent columns is $\mathbf{A}^\dagger = (\mathbf{A}^* \mathbf{A})^{-1} \mathbf{A}^*$. $\mathbb{E}\{\cdot\}$ denotes expectation. $|\cdot|$ denotes the cardinality of a set.

II. SYSTEM DESCRIPTION AND ASSUMPTIONS

Consider the network model shown in Figure 1. The base stations are represented by an independent homogeneous PPP Π_b of density λ_b . The mobile users are located according to an independent point process Π_u . The cells of the base stations form a Voronoi tessellation of the plane with respect to the process Π_b , and the users are connected to their closest base station. We assume that the density of the mobile process is sufficiently large such that all the base stations are active. Each base station is equipped with N_t antennas and serves one single antenna mobile user in each cell using intra-cell time division multiple access (TDMA). While TDMA is not necessarily the best option for a multiple-input-single-output (MISO) transmission strategy, it is a common assumption made in the multicell cooperation literature due to the tractability of single-user transmission [1], [13], [4], [19].

To model clustering, we overlay another independent homogeneous PPP Π_c on the 2-D plane with intensity $\lambda_c \leq \lambda_b$. We denote the cluster centers of this PPP by c_k . The cluster cells form a Voronoi tessellation of the plane with respect to the process Π_c . The base stations of the Π_b process located in the same Voronoi cell $V^{(c_k)}$ of a cluster center c_k coordinate via ICIN. The association of the base stations to the cluster base stations follows similar to the association of the mobile users to their closest base station in the basic cellular model. The cluster base stations can be seen as central processors to which base stations in the same cluster are connected via backhaul. The backhaul is assumed error and delay free.

Based on the stationarity of the Poisson process [23], we consider the performance for a typical user u_0 served by a base station b_0 inside a cluster $V^{(c_0)}(b_0)$. The channel corresponding to the desired signal between b_0 and u_0 is denoted by $\mathbf{h}_0^* \in \mathbb{C}^{1 \times N_t}$. The interfering channels from the ℓ -th base station to u_0 are denoted by $\mathbf{g}_{0,\ell}^* \in \mathbb{C}^{1 \times N_t}$. The

desired and interfering channels are modeled according to the Rayleigh fading model, where each entry is independently and identically distributed as a unit variance zero mean complex Gaussian. The symbol transmitted from the k -th base station is denoted by s_k , where $\mathbb{E}[|s_k|^2] = E_s$ and there is no power control. While power control is an important topic for practical networks, an exhaustive investigation of the topic would require a detailed analysis of a distributed power control algorithm among the base stations. Another way of implementing power control independently at each base station is to perform channel inversion and assume fixed received power [24]. Such a strategy leads to better outage performance for full CSI [19]. In the absence of interference coordination, each user is subject to interference from all other base stations in Π_b , each transmitting with energy E_s . The path-loss incurred by the desired signal is given by $L(r_0) = (1 + r_0)^\alpha$ where r_0 is the distance between u_0 and b_0 , and α is the path-loss exponent. For the interfering signals from the ℓ -th base station to u_0 , the path-loss is given by $L(r_{0,\ell}) = (1 + r_{0,\ell})^\alpha$, $r_{0,\ell} > r_0$. Most of the literature on analysis of random spatial models [16], [19] consider the $L(r) = r^\alpha$ path-loss model; this model, however, has a singularity at zero and is inaccurate for small distances. The received signal powers of the desired and interfering signals are then given by $\gamma_0 = E_s/L(r_0)$ and $\gamma_{0,\ell} = E_s/L(r_{0,\ell})$. Using a narrowband flat-fading model, the baseband discrete-time input-output relation for u_0 is given by

$$y_0 = \sqrt{\gamma_0} \mathbf{h}_0^* \mathbf{f}_0 s_0 + \sum_{b_\ell \in \Pi_b/b_0} \sqrt{\gamma_{0,\ell}} \mathbf{g}_{0,\ell}^* \mathbf{f}_\ell s_\ell + v_0, \quad (1)$$

where y_0 is the received signal at u_0 , the vector $\mathbf{f}_0 \in \mathbb{C}^{N_t \times 1}$ is the unit-norm beamforming vector at b_0 , and $\mathbf{f}_\ell \in \mathbb{C}^{N_t \times 1}$ is the unit-norm beamforming vector at the ℓ -th base station. The scalar v_0 denotes the additive white Gaussian noise at the receiver with variance σ^2 .

The signal-to-interference-plus-noise ratio (SINR) at u_0 is given by

$$\text{SINR}_0 = \frac{\gamma_0 |\mathbf{h}_0^* \mathbf{f}_0|^2}{\sigma^2 + \sum_{b_\ell \in \Pi_b/b_0} \gamma_{0,\ell} |\mathbf{g}_{0,\ell}^* \mathbf{f}_\ell|^2}. \quad (2)$$

For a given SINR threshold T , a performance metric of interest is the probability of coverage,

$$p_c(\lambda_b, \lambda_c, \alpha, T) = \mathbb{P}[\text{SINR}_0 \geq T]. \quad (3)$$

The probability of coverage is the probability that a randomly chosen user in the 2-D plane has a target SINR greater than T . Such a condition is required in practice when a given constant bit-rate corresponding to a particular coding scheme needs to be sustained.

Another performance metric of interest is the average rate,

$$\tau(\lambda_b, \lambda_c, \alpha) = \mathbb{E} \{\log_2 (1 + \text{SINR}_0)\}. \quad (4)$$

To express the average rate, we assume that adaptive modulation/coding is used so that the users achieve a Shannon bound for their rate.

III. PER CLUSTER INTERFERENCE COORDINATION

We propose interference coordination within each cluster based on zero forcing (ZF) intercell interference nulling. We assume there are N interfering base stations in the cluster of interest. Since N is a random variable that depends on λ_c and λ_b , the number of antennas at the base stations needs to be sufficiently high ($N_t > N$) for ICIN to be feasible inside each cluster. We assume for the first part of this paper that N_t grows with N such that $N_t - N = d_{N_t}$, where d_{N_t} are the extra degrees of freedom at each base station, used to beamform to the desired user [25], [26]. This assumption is relaxed to a preset constant N_t in Section VI. Each base station in the cluster has knowledge not only of the channel to its intended receiver, but also of the interference channels towards the receivers in the same cluster. Without loss of generality, for the case of the typical user, u_0 estimates its desired channel \mathbf{h}_0 and the interfering channels $\mathbf{g}_{0,\ell}$, $\ell = 1, \dots, N$, and feeds the information back to its base station b_0 . The base stations in the coordination cluster then exchange the interfering CSI on the backhaul, so that b_0 has knowledge of \mathbf{h}_0 and the interference channels towards other receivers in the cluster $\mathbf{g}_{\ell,0}$, $\ell = 1, \dots, N$,

We assume that perfect CSI is available at the receivers. Accounting for imperfections due to channels downlink training further degrades the achievable rate with imperfect CSI, and is a subject of future investigation. We consider first the ideal case where full CSI is available at the transmitters, we then discuss finite rate feedback.

A. ICIN with Perfect CSI

With perfect CSI at the transmitters, each base station designs its beamforming vector such that it is the normalized projection of the desired channel direction onto the null space of the matrix of interfering channel directions. For b_0 , \mathbf{f}_0 is the normalized projection of $\tilde{\mathbf{h}}_0 = \mathbf{h}_0 / \|\mathbf{h}_0\|$ onto the null space of $\mathbf{G}_{I,0} = [\tilde{\mathbf{g}}_{1,0} \cdots \tilde{\mathbf{g}}_{\ell,0} \cdots \tilde{\mathbf{g}}_{N,0}]$, with $\tilde{\mathbf{g}}_{\ell,0} = \mathbf{g}_{\ell,0} / \|\mathbf{g}_{\ell,0}\|$,

$$\mathbf{f}_0 = \frac{(\mathbf{I} - \mathbf{G}_{I,0} \mathbf{G}_{I,0}^\dagger) \tilde{\mathbf{h}}_0}{\|(\mathbf{I} - \mathbf{G}_{I,0} \mathbf{G}_{I,0}^\dagger) \tilde{\mathbf{h}}_0\|}. \quad (5)$$

The SINR_0 with per cluster ICIN, is given by

$$\begin{aligned} \text{SINR}_{ic} &= \frac{\gamma_0 |\mathbf{h}_0^* \mathbf{f}_0|^2}{\sum_{b_\ell \in \Pi_b/V^{(c_0)}(b_0)} \gamma_{0,\ell} |\mathbf{g}_{0,\ell}^* \mathbf{f}_\ell|^2 + \sigma^2} \\ &= \frac{(1 + r_0)^{-\alpha} |\mathbf{h}_0^* \mathbf{f}_0|^2}{I_{\text{out}} + 1/\text{SNR}}, \end{aligned} \quad (6)$$

where I_{out} is the inter-cluster interference caused by all the base stations outside the cluster of interest $V^{(c_0)}(b_0)$, denoted by $\Pi_b/V^{(c_0)}(b_0)$. The signal-to-noise-ratio (SNR) here is defined in terms of the transmit signal power, $1/\text{SNR} = \sigma^2/E_s$.

B. ICIN with Limited Feedback CSI

With limited feedback, the estimated channel directions $\tilde{\mathbf{h}}_0$ and $\tilde{\mathbf{g}}_{0,\ell}$ are quantized to the unit-norm vectors given by $\hat{\mathbf{h}}_0$ and $\hat{\mathbf{g}}_{0,\ell}$, respectively, at u_0 . These quantized channel

directions are then fed back to the base stations using a fixed feedback budget of B_{tot} bits. The base stations use these quantized channel directions to design the beamforming vector. We assume that the base stations have perfect knowledge of the SNR at the receivers, independently of the channel directions. Perfect non-quantized knowledge of the received SNR at the base stations is a common assumption in the literature on multi-user and multicell limited feedback [13], [27].

We consider separate quantization at the receiver of the desired and interfering signals. Joint quantization was considered in [28]; it requires a large storage space at the mobile users. Each user divides B_{tot} among the desired and interfering channels such that B_0 and $B_{0,\ell}$ are used to quantize $\hat{\mathbf{h}}_0$ and $\hat{\mathbf{g}}_{0,\ell}$ respectively, and $B_0 + \sum_{\ell=1}^N B_{0,\ell} = B_{\text{tot}}$ bits. We ignore delays on the feedback channel as well as delays on the backhaul link between the base stations belonging to the same cluster. The beamforming vector $\hat{\mathbf{f}}_0$ is the normalized projection of the quantized channel $\hat{\mathbf{h}}_0$ onto the null space of the matrix $\hat{\mathbf{G}}_{I,0} = [\hat{\mathbf{g}}_{1,0} \cdots \hat{\mathbf{g}}_{\ell,0} \cdots \hat{\mathbf{g}}_{N,0}]$,

$$\hat{\mathbf{f}}_0 = \frac{(\mathbf{I} - \hat{\mathbf{G}}_{I,0} \hat{\mathbf{G}}_{I,0}^\dagger) \hat{\mathbf{h}}_0}{\|(\mathbf{I} - \hat{\mathbf{G}}_{I,0} \hat{\mathbf{G}}_{I,0}^\dagger) \hat{\mathbf{h}}_0\|}. \quad (7)$$

SINR_0 with limited feedback and per cluster ICIN, is given by

$$\widehat{\text{SINR}}_{\text{ic}} = \frac{(1 + r_0)^{-\alpha} |\mathbf{h}_0^* \hat{\mathbf{f}}_0|^2}{\frac{1}{\text{SNR}} + \hat{I}_{\text{out}} + I_{\text{res}}},$$

where $I_{\text{res}} = \sum_{b_\ell \in V^{(c_0)}(b_0)/b_0} (1 + r_{0,\ell})^{-\alpha} |\mathbf{g}_{0,\ell}^* \hat{\mathbf{f}}_\ell|^2$ is the residual intra-cluster interference due to quantization. Interference signals are not nulled out, since $\mathbf{g}_{0,\ell}^* \hat{\mathbf{f}}_\ell \neq 0$ but $\hat{\mathbf{g}}_{0,\ell}^* \hat{\mathbf{f}}_\ell = 0$. $\hat{I}_{\text{out}} = \sum_{b_\ell \in \Pi_b/V^{(c_0)}(b_0)} (1 + r_{0,\ell})^{-\alpha} |\mathbf{g}_{0,\ell}^* \hat{\mathbf{f}}_\ell|^2$ is the inter-cluster interference assuming limited feedback beamforming.

We derive the average rate with perfect CSI in Section IV. We then bound the mean loss in rate with limited feedback for equal bit and adaptive bit partitioning among the desired and interfering channels in Section V.

IV. PERFORMANCE EVALUATION WITH PERFECT CSI

In this section, we analyze the outage performance of per cluster ICIN. We then use the probability of coverage expression to derive a bound on the average rate.

A. Probability of Coverage Analysis

The probability of coverage is the complementary cumulative distribution (CCDF) of SINR_{ic} ,

$$\begin{aligned} p_c(\lambda_b, \lambda_c, \alpha, T) &= \mathbb{P}[\text{SINR}_{\text{ic}} \geq T] \\ &= \mathbb{P}[|\mathbf{h}_0^* \mathbf{f}_0|^2 \geq TL(r_0)(I_{\text{out}} + 1/\text{SNR})]. \end{aligned} \quad (8)$$

The desired effective channel power $|\mathbf{h}_0^* \mathbf{f}_0|^2$ is Gamma-distributed with parameters d_{N_t} and 1, $|\mathbf{h}_0^* \mathbf{f}_0|^2 \sim \Gamma[d_{N_t}, 1]$. This follows from the projection of the independent normal Gaussian isotropic vector \mathbf{h}_0 onto the null space of the interfering channels of dimension $d_{N_t} = N_t - N$ [21], [25].

The aggregate inter-cluster interference power I_{out} is a function of the cluster size. While a numerical fit of the distribution of the cluster size is possible [29], an expression for the exact size of the Voronoi region $V^{(c_0)}(b_0)$ is hard to compute. Hence, we bound the area of the cluster of interest by the area of the maximal disk B_m inscribed in the cluster, and centered at c_0 . Let r_m designate the radius of B_m . r_m is Rayleigh distributed with CCDF $\mathbb{P}[r_m > r] = \exp(-4\pi\lambda_c r^2)$, [30]. The interference power is then upper bounded by

$$\begin{aligned} I_{\text{out}} &= \sum_{\Pi_b/V^{(c)}(b_0)} \gamma_{0,\ell} |\mathbf{g}_{0,\ell}^* \mathbf{f}_\ell|^2 \leq \sum_{\Pi_b/B_m} \gamma_{0,\ell} |\mathbf{g}_{0,\ell}^* \mathbf{f}_\ell|^2 \\ &\leq \sum_{\Pi_b/B_m(u_0)} \gamma_{0,\ell} |\mathbf{g}_{0,\ell}^* \mathbf{f}_\ell|^2, \end{aligned} \quad (9)$$

where $B_m(u_0)$ denotes the disk centered at the typical mobile user u_0 of radius $r_m - r_0 - r_1$, where r_1 is the distance from b_0 to c_0 , Rayleigh distributed with probability density function (PDF) $f_{r_1}(r) = 2\pi\lambda_c r \exp(-\pi\lambda_c r^2)$. The interference field power is computed at u_0 located at a distance $0 \leq r \leq r_m$ from the center of the inscribed disk B_m corresponding to the cluster-cell center. The exclusion distance to the nearest interferer from the mobile user is asymmetric since the distance from the mobile user to the closest edge of the disk is smaller than its distance from the furthest edge. To avoid the dependence on the location of the interference field, we pursue an upper bound on the interference power. We consider the interference contribution in a disk of radius $r_m - r_1 - r_0$ centered at u_0 and denoted by $B_m(u_0)$. The exclusion areas are such that $B_m(u_0) \subseteq B_m \subseteq V^{(c_0)}(b_0)$. The upper bound on the aggregate inter-cluster interference power results in a lower bound on the probability of coverage.

Result 1: The probability of coverage with per cluster interference coordination is lower bounded by

$$\begin{aligned} p_{c,\text{ic}}(\lambda_b, \lambda_c, \alpha, T) &\geq \left\{ \int_0^\infty f_r(r_0) \int_{r_0}^\infty f_{r_m}(r_m) \times \right. \\ &\quad \left. \int_{-\infty}^\infty e^{-2\pi j \frac{TL(r_0)}{\text{SNR}} s} \mathcal{L}_{I_{r_m}}(2j\pi L(r_0)Ts) \frac{\mathcal{L}_h(-2j\pi s) - 1}{2i\pi s} ds dr_0 dr_m \right\}, \end{aligned} \quad (10)$$

where the Laplace transform of the desired signal $|\mathbf{h}_0^* \mathbf{f}_0|^2 \sim \Gamma[d_{N_t}, 1]$, is

$$\mathcal{L}_h(s) = \frac{1}{(s+1)^{d_{N_t}}}, \quad d_{N_t} = N_t - N.$$

The PDF of r_0 , $f_r(r) = 2\pi\lambda_b r \exp(-\pi\lambda_b r^2)$, follows from the null probability of a 2-D PPP with respect to Π_b . The PDF of the radius r_m is $f_{r_m}(r) = 8\pi\lambda_c r \exp(-4\pi\lambda_c r^2)$. The Laplace transform of the interference \mathcal{L}_{I_r} is

$$\begin{aligned} \mathcal{L}_{I_r}(s) &= \\ &\exp \left\{ -2\pi\lambda_b \left(\frac{(1+r)^{2-\alpha}}{\alpha-2} s {}_2F_1 \left(1, 1 - \frac{2}{\alpha}, 2 - \frac{2}{\alpha}, -(1+r)^{-\alpha} s \right) \right. \right. \\ &\quad \left. \left. - \frac{(1+r)^{1-\alpha}}{\alpha-1} s {}_2F_1 \left(1, 1 - \frac{1}{\alpha}, 2 - \frac{1}{\alpha}, -(1+r)^{-\alpha} s \right) \right) \right\}, \end{aligned} \quad (11)$$

where ${}_2F_1(a, b, c, z) = \frac{\Gamma(c)}{\Gamma(b)\Gamma(c-b)} \int_0^1 \frac{t^{b-1}(1-t)^{c-b-1}}{(1-tz)^a} dt$ denotes the Gauss hypergeometric function.

Proof: See Appendix A. ■

The tightness of the upper bound on the probability of outage is investigated in Section VII. The probability of coverage depends on the density of interfering base stations, the density of the clusters, the path-loss exponent and the number of extra spatial dimensions available at the transmitters d_{N_t} . It is an increasing function of the ratio of the density of interfering base stations to the density of the cluster base stations λ_b/λ_c , which is also the average number of base stations per cluster. It is also an increasing function of d_{N_t} . As N_t increases, d_{N_t} increases, and the signal power at the mobile users increases, which incurs an increase in the SINR, in addition to the decrease in the interference term due to ICIN per cluster.

B. Average Rate

The average rate follows from the probability of coverage analysis as follows

$$\tau = \mathbb{E} \{ \log_2(1 + \text{SINR}_0) \} = \int_0^\infty \frac{\mathbb{P}[\text{SINR}_0 > e^t - 1]}{\log(2)} dt. \quad (12)$$

Inserting (10) into (12) gives a lower bound on the average rate of the typical user.

Result 2: The throughput of the typical user u_0 , averaged over the spatial realizations of the point processes Π_b and Π_c , and the channel fading distributions is bounded by

$$\begin{aligned} \tau_{ic}(\lambda_b, \lambda_c, \alpha) &= \int_0^\infty \frac{\mathbb{P}[\text{SINR}_{ic} > e^t - 1]}{\log(2)} dt \\ &= \int_0^\infty \frac{p_{c,ic}(\lambda_b, \lambda_c, \alpha, v)}{(1+v)\log(2)} dv \\ &\geq \int_0^\infty \frac{p_{c,ic}^{lb}(\lambda_b, \lambda_c, \alpha, v)}{(1+v)\log(2)} dv, \end{aligned} \quad (13)$$

where $p_{c,ic}^{lb}(\lambda_b, \lambda_c, \alpha, v)$ is the lower bound on the probability of coverage $p_{c,ic}(\lambda_b, \lambda_c, \alpha, v)$ on the right hand side of (10).

The computation of τ_{ic} requires an additional numerical integration over $p_{c,ic}$. As in the case of coverage, τ_{ic} depends on the average cluster size. It increases with increasing d_{N_t} and increasing λ_b/λ_c , as illustrated in Section VII.

V. IMPACT OF LIMITED FEEDBACK ON AVERAGE RATE

The performance of ICIN depends on the availability of accurate channel state information at the cooperating base stations. With limited feedback, the quantized CSI is fed back from the receiver to the transmitter. The feedback resources at each mobile user are partitioned among the desired and interfering channels. The bit allocation strategy between the quantized channels is hence important to minimize the mean loss in rate due to limited feedback.

We compute an upper bound on the mean loss in rate using limited feedback. We use separate codebooks to quantize each desired and interfering channel. We consider random vector quantization in which each of the quantization vectors is independently chosen from the isotropic distribution on the N_t dimensional unit sphere [31]. RVQ is chosen because it is amenable to analysis and yields tractable bounds on the mean loss in rate. Furthermore, optimum codebooks are not yet known for multicell cooperative transmission [13].

We define the mean loss in rate due to limited feedback as

$$\Delta \hat{\tau}_{ic} = \mathbb{E} \left\{ \log_2(1 + \text{SINR}_{ic}) \right\} - \mathbb{E} \left\{ \log_2(1 + \widehat{\text{SINR}}_{ic}) \right\} = \tau_{ic} - \hat{\tau}_{ic}, \quad (14)$$

where $\hat{\tau}_{ic}$ is the average rate with limited feedback¹.

The SINRs with perfect and limited feedback CSI are such that $\text{SINR}_{ic} \geq \widehat{\text{SINR}}_{ic}$. Subsequently $\log_2(1 + \text{SINR}_{ic}) - \log_2(1 + \widehat{\text{SINR}}_{ic}) \leq \log_2(\text{SINR}_{ic}) - \log_2(\widehat{\text{SINR}}_{ic})$ and

$$\Delta \hat{\tau}_{ic} \leq \mathbb{E} \{ \log_2(\text{SINR}_{ic}) - \log_2(\widehat{\text{SINR}}_{ic}) \}. \quad (15)$$

We denote the upper bound on $\Delta \hat{\tau}_{ic}$ by $\Delta \hat{\tau}_{ic}^{\text{ub}}$ given by

$$\Delta \hat{\tau}_{ic}^{\text{ub}} = \underbrace{\mathbb{E} \left\{ \log_2 \left(\frac{|\tilde{\mathbf{h}}_0^* \mathbf{f}_0|^2}{|\tilde{\mathbf{h}}_0^* \hat{\mathbf{f}}_0|^2} \right) \right\}}_{\Delta \hat{\tau}_{\text{des}}} + \underbrace{\mathbb{E} \left\{ \log_2 \left(\frac{\hat{I}_{\text{out}} + \frac{1}{\text{SNR}} + I_{\text{res}}}{I_{\text{out}} + \frac{1}{\text{SNR}}} \right) \right\}}_{\Delta \hat{\tau}_{\text{int}}},$$

where $\Delta \hat{\tau}_{\text{des}}$ denotes the mean loss from quantizing the desired channel and $\Delta \hat{\tau}_{\text{int}}$ is the mean loss from quantizing the interference channels.

To derive the contribution of the desired signal quantization, $\Delta \hat{\tau}_{\text{des}}$, we use a lower bound on the desired signal power with limited feedback, [13]

$$\begin{aligned} \mathbb{E} \{ \log_2(|\mathbf{h}_0^* \hat{\mathbf{f}}_0|^2) \} &\geq -\mathbb{E}_N \left\{ \frac{\log_2(e)}{N_t - 1} \sum_{i=1}^{N_t-1} \beta \left(2^{B_0}, \frac{i}{N_t - 1} \right) \right\} \\ &\quad + \mathbb{E} \left[\log_2(\|\mathbf{h}_0\|^2 |\hat{\mathbf{h}}_0^* \hat{\mathbf{f}}_0|^2) \right]. \end{aligned} \quad (16)$$

An upper bound on $\Delta \hat{\tau}_{\text{des}}$ then follows

$$\Delta \hat{\tau}_{\text{des}} \leq \log_2(e) \mathbb{E}_N \left\{ \frac{1}{N_t - 1} \sum_{i=1}^{N_t-1} \beta \left(2^{B_0}, \frac{i}{N_t - 1} \right) \right\} \quad (17)$$

since $\mathbb{E} \left\{ \log_2(\|\mathbf{h}_0\|^2 |\hat{\mathbf{h}}_0^* \hat{\mathbf{f}}_0|^2) \right\} = \mathbb{E} \left\{ \log_2(\|\mathbf{h}_0\|^2 |\mathbf{h}_0^* \mathbf{f}_0|^2) \right\}$. The Beta function is defined as $\beta(a, b) = \int_0^1 t^{a-1} (1-t)^{b-1} dt$.

The effective interference power from each base station outside the cluster is a function of the interference channels towards the typical user, and the quantization vector $\hat{\mathbf{f}}_\ell$. The quantization vector is independent of $\mathbf{g}_{0,\ell}^*$ and is computed using RVQ. The interference power from each base station is thus distributed as $|\mathbf{g}_{0,\ell}^* \hat{\mathbf{f}}_\ell|^2 \sim \Gamma[1, 1]$, $\ell = 1, \dots, N$, [24], [31]. We rewrite $\Delta \hat{\tau}_{\text{int}}$ as

$$\Delta \hat{\tau}_{\text{int}} = \mathbb{E} \left\{ \log_2 \left(I_{\text{out}} + \frac{1}{\text{SNR}} + I_{\text{res}} \right) - \log_2 \left(I_{\text{out}} + \frac{1}{\text{SNR}} \right) \right\},$$

and we focus hereafter on the effect of the residual intra-cluster interference I_{res} .

The statistics of I_{res} and the bound on the mean loss in rate depends on the number of interfering base stations inside the cluster N , and the strategy of allocating bits among the desired and interfering channels. We first consider an equal bit allocation strategy, independent of the channels' strength, we

¹ $\mathbb{E} \left\{ \log_2(1 + \widehat{\text{SINR}}_{ic}) \right\}$ is an upper bound on the achievable rate with limited feedback [32]. This bound is approached when the mobile user has perfect knowledge of the coupling coefficients between the beamforming vectors used at the base stations and the channel vectors [32].

then optimize the bit allocation to minimize the mean loss in rate.

A. Equal Bit Allocation

One option for bit allocation is to divide B_{tot} almost equally between the interfering channels and the desired channel, that is $B_{0,\ell} = \lfloor B_{\text{tot}}/(N+1) \rfloor$ and then set $B_0 = B_{\text{tot}} - NB_{0,\ell}$. This is a suboptimal strategy because it does not account for the difference in the path-loss between the various interferers, and hence the difference in the importance of the interfering signals. It gives, however, a slight bias for quantizing the desired channel, when the number of bits is not a multiple of the number of base stations in the cluster. In this section, we compute a closed form expression for the bound on the mean loss in rate, and we use it as a stepping stone to later optimize the bit allocation.

The bound on the mean loss in rate is rewritten as

$$\begin{aligned} \Delta \hat{\tau}_{\text{ic}}^{\text{ub}} &\leq \log_2(e) \mathbb{E}_N \left\{ \frac{1}{N_t - 1} \sum_{i=1}^{N_t-1} \beta \left(2^{B_0}, \frac{i}{N_t - 1} \right) \right\} \\ &\quad - \mathbb{E} \left\{ \log_2(I_{\text{out}} + 1/\text{SNR}) \right\} \\ &\quad + \mathbb{E} \left\{ \log_2 \left(\sum_{\ell=1}^N (1 + r_{0,\ell})^{-\alpha} |\mathbf{g}_{0,\ell}^* \hat{\mathbf{f}}_\ell|^2 + I_{\text{out}} + 1/\text{SNR} \right) \right\}. \end{aligned}$$

As $\Delta \hat{\tau}_{\text{ic}}^{\text{ub}}$ is averaged over all the spatial realizations in the network, with different number of interferers N , we first derive the probability mass function (PMF) of N in a typical cluster. The PMF of N depends on the cluster size. It is the distribution of the number of points inside a cluster area, given that a randomly chosen point is located in that area.

Lemma 1: The probability mass function of the number of interferers N inside the cluster of interest is given by

$$\mathbb{P}[N = n] = \frac{3.5^{4.5} \Gamma(n + 4.5) (\lambda_b/\lambda_c)^n}{\Gamma(4.5) n! (\lambda_b/\lambda_c + 3.5)^{n+4.5}}, \quad (18)$$

Proof: See Appendix B. ■

For the contribution of the inter-cluster interference I_{out} and consequently I_{r_m} in $\Delta \hat{\tau}_{\text{ic}}^{\text{ub}}$, we approximate the distribution of I_{r_m} with the Gamma distribution, using second-order moment matching [33]. The Gamma approximation yields more tractable expressions for $\mathbb{E}\{\log(I_{r_m})\}$ than the challenging to compute density and Laplace characterizations of I_{r_m} .

Remark 1: (Gamma Distribution Second Order Moment Matching) For the second-order moment matching of the Gamma random variable, consider a random variable x with finite first $\mathbb{E}\{x\}$ and second order $\mathbb{E}\{x^2\}$ moments, and variance $\text{var}(x) = \mathbb{E}\{x^2\} - (\mathbb{E}\{x\})^2$. The Gamma distribution $\Gamma[k, \theta]$ with the same first and second order moments as x has parameters $k = \frac{(\mathbb{E}\{x\})^2}{\text{var}(x)}$, and $\theta = \frac{\text{var}(x)}{\mathbb{E}\{x\}}$.

For the residual intra-cluster interference, we invoke Jensen's inequality on the first term on the right hand side of (18) to derive a closed form expression for $\mathbb{E}\{I_{\text{res}}\}$

$$\begin{aligned} \mathbb{E}\{I_{\text{res}}\} &= \mathbb{E} \left\{ \sum_{\ell=1}^N (1 + r_{0,\ell})^{-\alpha} |\mathbf{g}_{0,\ell}^* \hat{\mathbf{f}}_\ell|^2 \right\} \\ &= \mathbb{E}_{N,r_{0,\ell}} \left\{ \sum_{\ell=1}^N (1 + r_{0,\ell})^{-\alpha} \mathbb{E} \left\{ |\mathbf{g}_{0,\ell}^* \hat{\mathbf{f}}_\ell|^2 \right\} \right\} \\ &\stackrel{(a)}{=} \mathbb{E}_{N,r_{0,\ell}} \left\{ \sum_{\ell=1}^N (1 + r_{0,\ell})^{-\alpha} \frac{N_t}{N_t - 1} 2^{B_{0,\ell}} \beta \left(2^{B_{0,\ell}}, \frac{N_t}{N_t - 1} \right) \right\} \\ &\stackrel{(b)}{=} \mathbb{E}_{N,r_{0,\ell}} \left\{ \sum_{\ell=1}^N (1 + r_{0,\ell})^{-\alpha} \Gamma \left(\frac{2N_t - 1}{N_t - 1} \right) 2^{-\frac{B_{0,\ell}}{N_t - 1}} \right\}, \end{aligned}$$

where (a) follows from using RVQ for quantization $\mathbb{E}\{|\mathbf{g}_{0,\ell}^* \hat{\mathbf{f}}_\ell|^2\} = \frac{N_t}{N_t - 1} 2^{B_{0,\ell}} \beta \left(2^{B_{0,\ell}}, \frac{N_t}{N_t - 1} \right)$, [13], [31]. (b) follows from Stirling's approximation on the Beta function.

Result 3: The mean loss in rate from limited feedback with ICIN, with equal bit allocation, is bounded by

$$\begin{aligned} \Delta \hat{\tau}_{\text{ic}} &\leq \log_2(e) \sum_{n=0}^{\infty} \Gamma \left(\frac{N_t}{N_t - 1} \right) 2^{-\frac{B_{\text{tot}} - n \lfloor \frac{B_{\text{tot}}}{N_t - 1} \rfloor}{N_t - 1}} P_N(n) \\ &\quad - \log_2(e) \psi(k) - \log_2(\theta) + \log_2 \left(1/\text{SNR} + k\theta \right) \\ &\quad + \sum_{n=0}^{\infty} n \Gamma \left(\frac{2N_t - 1}{N_t - 1} \right) 2^{-\lfloor \frac{B_{\text{tot}}}{N_t - 1} \rfloor \frac{1}{N_t - 1}} P_N(n) \mathbb{E}\{(1 + r_{0,1})^{-\alpha}\}, \end{aligned}$$

where

$$\mathbb{E}\{(1 + r_{0,1})^{-\alpha}\} = \int_0^\infty \int_{r_0}^\infty (1 + r)^{-\alpha} \frac{r}{2\pi\lambda_b} e^{-\frac{r^2}{4\pi\lambda_b}} f_{r_0}(r_0) dr dr_0,$$

and $I_{\text{out}} \sim \Gamma[k, \theta]$ via second-order moment matching [33], with parameters k and θ such that $\mathbb{E}\{I_{r_m}\} = k\theta$ and $\text{var}(I_{r_m}) = k\theta^2$, with

$$\mathbb{E}\{I_{r_m}\} = 2\pi\lambda_b \mathbb{E}_{r_m,r_0} \left\{ \int_{r_m-r_0}^\infty \frac{r}{L(r)} dr \right\} \text{ and } \text{var}(I_{r_m}) = 2\pi\lambda_b \mathbb{E}_{r_m,r_0} \left\{ \int_{r_m-r_0}^\infty \frac{r}{(L(r))^2} dr \right\}.$$

Proof: See Appendix C. ■

The mean loss in rate $\Delta \hat{\tau}_{\text{ic}}$ decreases as the total number of bits B_{tot} increases. $\Delta \hat{\tau}_{\text{ic}}$ increases, however, with the average cluster size λ_b/λ_c , given a fixed feedback budget B_{tot} . A higher λ_b/λ_c implies more base stations per cluster and hence more interfering channels to quantize. As the number of antennas at the base stations increases with the number of base stations per cluster for ICIN to be feasible, the number of bits allocated per antenna for each quantized channel also decreases.

B. Adaptive Bit Allocation

As the equal bit allocation limited feedback strategy results in a considerable decrease in the ICIN performance, as will be illustrated in Section VII, in this section we optimize the bit allocation to minimize the mean loss in achievable rate of ICIN. We adapt the number of bits allocated to the desired and interfering channels as a function of their signal strength at the typical user. Since each spatial realization results in a different number of intra-cluster interferers N , the optimization is done per spatial realization, as a function of N .

We denote the total number of bits allocated to quantizing the interfering channels by $B_i = B_{\text{tot}} - B_0$. Given B_i , we

first derive $B_{0,\ell}, \ell = 1, \dots, N$ such that the contribution of the interfering channels towards the mean loss in rate is minimized. In other words, we aim at finding $B_{0,\ell}$ such that I_{res} is minimized. The optimization problem is expressed as

$$\min_{B_{0,1}, \dots, B_{0,N}} \sum_{\ell=1}^N (1+r_{0,\ell})^{-\alpha} \Gamma\left(\frac{2N_t-1}{N_t-1}\right) 2^{-\frac{B_{0,\ell}}{N_t-1}} \quad (19)$$

s.t. $\sum_{\ell=1}^N B_{0,\ell} = B_i$, and $B_{0,\ell} > 0$.

The bit allocations $B_{0,\ell}, \ell \in 1 \dots N$ are integer-valued. We solve a relaxation of the optimization problem assuming $B_{0,\ell}$ are real valued. The solution is given by the arithmetic-geometric mean inequality. It is derived in [13] and restated here for completeness.

Lemma 2: ([13, Theorem 4]) The optimum number of bits assigned to the ℓ -th interferer, $B_{0,\ell}^*$, that minimizes (19) is given by

$$B_{0,\ell}^* = \frac{B_i}{|\mathcal{K}|} + (N_t - 1) \log_2 \left(\frac{(1+r_{0,\ell})^{-\alpha}}{\prod_{\ell \in \mathcal{K}} (1+r_{0,\ell})^{-\alpha/|\mathcal{K}|}} \right) \quad (20)$$

for $\ell \in \mathcal{K}$ and $B_{0,\ell} = 0$ for $\ell \notin \mathcal{K}$, where \mathcal{K} is the largest set of interferers that satisfies

$$\log_2 \left(\frac{\prod_{\ell \in \mathcal{K}} (1+r_{0,\ell})^{-\alpha/|\mathcal{K}|}}{(1+r_{0,\ell})^{-\alpha}} \right) < \frac{B_i}{|\mathcal{K}|(N_t-1)}. \quad (21)$$

\mathcal{K} denotes the set of effective interferers, such that $|\mathcal{K}| \leq N$. Using the expression for $B_{0,\ell}$ from (20), the bound on the mean loss in rate per spatial realization, i.e. given N and $r_{0,\ell}$ is expressed as a function of a single variable $B_0 = B_{\text{tot}} - B_i$,

$$\begin{aligned} \Delta \hat{\tau}_{\text{ic}}(B_0) &\approx \log_2(e) \Gamma\left(\frac{N_t}{N_t-1}\right) 2^{-\frac{B_0}{N_t-1}} \\ &- \mathbb{E} \left\{ \log_2(I_{\text{out}} + 1/\text{SNR}) \right\} \\ &+ \log_2 \left(\Gamma\left(\frac{2N_t-1}{N_t-1}\right) |\mathcal{K}| 2^{-\frac{B_{\text{tot}}-B_0}{|\mathcal{K}|(N_t-1)}} \prod_{\ell \in \mathcal{K}} (1+r_{0,\ell})^{-\alpha/|\mathcal{K}|} \right. \\ &\quad \left. + \mathbb{E}\{I_{\text{out}}\} + 1/\text{SNR} \right). \end{aligned} \quad (22)$$

To minimize the mean loss in rate, we minimize $\Delta \hat{\tau}_{\text{ic}}(B_0)$ as a function of B_0 such that $B_0 \leq B_{\text{tot}}$. We distinguish between two cases of interest, depending on the ratio of residual interference I_{res} to inter-cluster interference I_{out} .

Dominant Inter-Cluster Interference: When $\mathbb{E}\{I_{\text{res}}\} < \mathbb{E}\{I_{\text{out}}\} + 1/\text{SNR}$, we use the low-SNR approximation $\log(1+x) \approx x$. The bound on the mean loss in rate is written as

$$\begin{aligned} \Delta \hat{\tau}_{\text{ic}}(B_0) &\approx \log_2(e) \Gamma\left(\frac{N_t}{N_t-1}\right) 2^{-\frac{B_0}{N_t-1}} \\ &- \mathbb{E} \left\{ \log_2(I_{\text{out}} + 1/\text{SNR}) \right\} + \log_2(\mathbb{E}\{I_{\text{out}}\} + 1/\text{SNR}) \\ &+ \log_2(e) \frac{\Gamma\left(\frac{2N_t-1}{N_t-1}\right)}{\mathbb{E}\{I_{\text{out}}\} + 1/\text{SNR}} |\mathcal{K}| 2^{-\frac{B_{\text{tot}}-B_0}{|\mathcal{K}|(N_t-1)}} \prod_{\ell \in \mathcal{K}} (1+r_{0,\ell})^{-\alpha/|\mathcal{K}|}. \end{aligned} \quad (23)$$

The optimization is carried out for the terms in B_0 .

Result 4: The optimal value of B_0 for $\mathbb{E}\{I_{\text{res}}\} < \mathbb{E}\{I_{\text{out}}\} + 1/\text{SNR}$, given N and $r_{0,\ell}, \ell = 1 \dots N$, is

$$\begin{aligned} B_0 &= \frac{B_{\text{tot}}}{|\mathcal{K}|+1} - \log_2 \left(\frac{N_t |\mathcal{K}|}{N_t-1} \prod_{\ell=1}^{|\mathcal{K}|} (1+r_{0,\ell})^{-\frac{\alpha}{|\mathcal{K}|}} \right) \frac{(N_t-1)|\mathcal{K}|}{|\mathcal{K}|+1} \\ &+ \log_2(\mathbb{E}\{I_{\text{out}}\} + 1/\text{SNR}) \frac{(N_t-1)|\mathcal{K}|}{|\mathcal{K}|+1}. \end{aligned} \quad (24)$$

Proof: The proof is provided in Appendix D. ■

Dominant Residual Intra-Cluster Interference When $\mathbb{E}\{I_{\text{res}}\} > \mathbb{E}\{I_{\text{out}}\} + 1/\text{SNR}$, we use the high SNR approximation $\log(1+x) \approx \log(x)$ and we write $\Delta \hat{\tau}_{\text{ic}}(B_0)$ as

$$\begin{aligned} \Delta \hat{\tau}_{\text{ic}}(B_0) &\approx \log_2(e) \Gamma\left(\frac{N_t}{N_t-1}\right) 2^{-\frac{B_0}{N_t-1}} - \mathbb{E} \left\{ \log_2(I_{\text{out}} + 1/\text{SNR}) \right\} \\ &+ \log_2 \left(\Gamma\left(\frac{2N_t-1}{N_t-1}\right) |\mathcal{K}| \prod_{\ell \in \mathcal{K}} (1+r_{0,\ell})^{-\alpha/|\mathcal{K}|} \right) + \frac{B_0 - B_{\text{tot}}}{|\mathcal{K}|(N_t-1)}. \end{aligned} \quad (25)$$

Since the terms which are a function of B_0 in (25) are convex with respect to B_0 , the optimal value of B_0 is found by taking the derivative of these terms with respect to B_0 .

Result 5: The optimal value of B_0 for $\mathbb{E}\{I_{\text{res}}\} > \mathbb{E}\{I_{\text{out}}\} + 1/\text{SNR}$, given N , is

$$B_0 = (N_t - 1) \log_2 \left(|\mathcal{K}| \log_2(e) \Gamma\left(\frac{N_t}{N_t-1}\right) \right). \quad (26)$$

The optimization problems for both dominant inter-cluster and dominant intra-cluster interference are solved assuming non-integer bit values. Since the objective functions in (23) and (25) are convex in B_0 , we get the integer value of B_0 by taking the floor or the ceiling of the value in (24) and (26), respectively.

An upper bound on mean loss in rate with adaptive bit allocations, averaged over all spatial realizations, is subsequently given by replacing B_0 by its optimal value in (23), distinguishing between the two dominant interference cases.

VI. PERFORMANCE EVALUATION WITH PERFECT CSI WITH FIXED N_t

In the analysis so far, we assumed that N_t is a function of the number of interferers in the cluster and hence is a random variable. This assumption makes the analysis with perfect and imperfect CSI more tractable, and allows system designers to gauge how many antennas they should provide at the base stations for interference coordination to be most beneficial.

In this section, since the number of antennas may be predetermined, we relax this assumption and we assume N_t is fixed at each base station. As N is a random variable that changes per spatial realization and can become greater than N_t , interference coordination may no longer be feasible per cluster. To overcome this issue, we propose a thresholding policy wherein if $N_t \leq N$, each base station beamforms to its own user and no interference coordination is performed. When $N_t > N$, ICIN is applied as in Section IV.

Let A be the event that the number of interferers in the cluster is less than N_t , then for a fixed N_t the probability of coverage is expressed as

$$\begin{aligned}
p_c(\lambda_b, \lambda_c, \alpha, N_t) &= \mathbb{P}[\text{SIR}_0 \geq T|A]\mathbb{P}[A] + \mathbb{P}[\text{SIR}_0 \geq T|A^c]\mathbb{P}[A^c] \\
&= \underbrace{\mathbb{P}[\text{SIR}_0 \geq T \cap A]}_{p_{c,ic}, N_t} + \underbrace{\mathbb{P}[\text{SIR}_0 \geq T \cap A^c]}_{p_{c,nic}, N_t}. \quad (27)
\end{aligned}$$

The probability of coverage with per cluster coordination and $N_t > N$ follows from the probability of coverage expression derived in Section IV with one difference being that the averaging is now done over N , given that N_t is fixed and the Laplace transform of the desired signal depends on $N_t - N$, now a random variable. Using the PMF of N in Section V, the lower bound on the probability of coverage $p_{c,ic}, N_t$ is

$$p_{c,ic}, N_t(\lambda_b, \lambda_c, \alpha, T) \geq \sum_{n=0}^{N_t-1} \left\{ p_N(n) \int_0^\infty f_r(r_0) \int_{r_0}^\infty f_{r_m}(r_m) \times \int_{-\infty}^\infty e^{-2\pi j \frac{L(r_0)T}{\text{SNR}} s} \mathcal{L}_{I_{r_m}}(2j\pi L(r_0)Ts) \frac{\mathcal{L}_h(-2j\pi s) - 1}{2i\pi s} ds dr_0 dr_m \right\},$$

where the desired signal $|\mathbf{h}_0^* \mathbf{f}_0|^2 \sim \Gamma[N_t - n, 1]$, and $p_N[n]$, $f_c(c)$ and $f_r(r_0)$ are given in (18) and Result 1, respectively.

With single-cell beamforming and no interference coordination, the interference at the typical user u_0 is divided into two independent components, the inter-cluster interference I_{out} bounded by I_{r_m} , and the intra-cluster interference denoted by I_{in} . The SINR, with perfect CSI beamforming, is given by where the desired signal power $\|\mathbf{h}_0\|^2 \sim \Gamma[1, N_t]$, and I_{out} and I_{in} are independent by the PPP property, since the interfering base stations are located in two disjoint areas.

The probability of coverage with beamforming, with $N_t < N$, is expressed as

$$\begin{aligned}
p_{c,nic}, N_t(\lambda_b, \lambda_c, \alpha, T) &= \\
\mathbb{E}_{N, r_0} \left\{ \mathbb{P}[\|\mathbf{h}\|^2 > L(r_0)T(I_{\text{out}} + I_{\text{in}} + 1/\text{SNR})] \right\}. \quad (29)
\end{aligned}$$

Conditioned on the value of N , the number of interferers inside the cluster is fixed, and the point process corresponding to the base stations interferers inside the cluster forms a binomial point process [34]. The intra-cluster interference term I_{in} is thus a result of a binomial point process in the area formed by the cluster. For the contribution of I_{in} , we compute an upper bound assuming the interference is the aggregation of the signal powers of the interfering base stations in the annular region with inner radius r_0 and outer radius r_M corresponding to the circumscribed circle to the cluster.

The probability of coverage with no interference nulling is

$$\begin{aligned}
p_{c,nic}, N_t &\geq \left\{ \sum_{n=N_t}^\infty \mathbb{P}[N = n] \int_0^\infty f_{r_0}(r_0) \int_{r_0}^\infty f_{r_m}(r_m) \int_{r_0}^\infty f_{r_M}(r_M) \right. \\
&\quad \times \int_{-\infty}^\infty e^{-2\pi j s / \text{SNR}} \mathcal{L}_{I_{r_m}}(2j\pi s) \mathcal{L}_{I_{r_M}}(2j\pi s) \\
&\quad \left. \frac{\mathcal{L}_h(-2j\pi(L(r_0)T)^{-1}s) - 1}{2j\pi s} ds dr_m dr_M dr_0 \right\},
\end{aligned}$$

where r_M is such that its CCDF is bounded by, [35]

$$\mathbb{P}[r_M > r] \geq 2\pi r^2 e^{-\pi r^2} (1 + \frac{1}{2\pi r^2} e^{-\pi r^2})$$

and the Laplace transform of I_{r_M} is given by

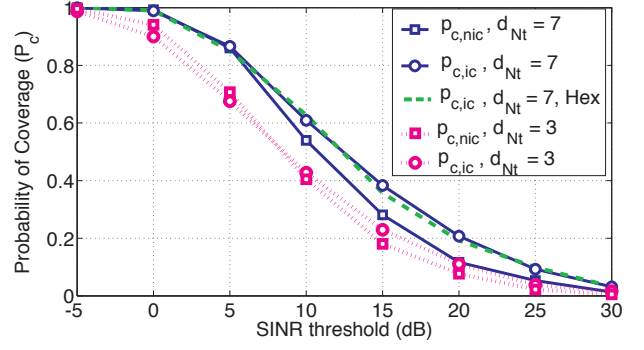


Fig. 2. The probability of coverage for increasing SINR threshold. $p_{c,ic}$ denotes the coverage with per cluster ICIN. $p_{c,nic}$ denotes the probability of coverage with beamforming and no nulling. The average number of base stations in the cell is 3 and the pathloss exponent is 4.

$$\begin{aligned}
L_{I_{r_M}}(s) &= \left\{ 1 - \frac{2\pi((r_0+1)(r_M+1))^{-\alpha}s}{\pi r_M^2 - \pi r_0^2} \times \left\{ \right. \right. \\
&\quad \frac{1}{\alpha-2} \left((r_0+1)^2 (r_M+1)^{\alpha} {}_2F_1\left(1, 1 - \frac{2}{\alpha}, 2 - \frac{2}{\alpha}, -(r_0+1)^{-\alpha}s\right) \right. \\
&\quad \left. \left. - (r_M+1)^2 (r_0+1)^{\alpha} {}_2F_1\left(1, 1 - \frac{2}{\alpha}, 2 - \frac{2}{\alpha}, -(r_M+1)^{-\alpha}s\right) \right) \right. \\
&\quad \left. + \frac{1}{\alpha-1} \left(-(r_0+1)(r_M+1)^{\alpha} {}_2F_1\left(1, 1 - \frac{1}{\alpha}, 2 - \frac{1}{\alpha}, -(r_0+1)^{-\alpha}s\right) \right. \right. \\
&\quad \left. \left. (r_M+1)(r_0+1)^{\alpha} {}_2F_1\left(1, 1 - \frac{1}{\alpha}, 2 - \frac{1}{\alpha}, -(r_M+1)^{-\alpha}s\right) \right) \right\}^N.
\end{aligned}$$

Combining the expressions for $p_{c,ic}, N_t$ and $p_{c,nic}, N_t$, we obtain the main result on the probability of coverage $p_{c,N_t}(\lambda_b, \lambda_c, \alpha, T)$ with interference coordination, for fixed N_t with thresholding.

The average throughput for fixed N_t follows from the probability of coverage analysis similarly to Section IV.

VII. SIMULATION RESULTS AND DISCUSSION

We consider a surface comprising on average 100 clusters. For random clustering, the density of the cluster base stations λ_c is varied such that $\lambda_c/\lambda_b \geq 1$ to show the benefits of increasing cluster sizes. The path-loss exponent is set to $\alpha = 4$.

Throughout the numerical evaluation, we compare the performance of per cluster ICIN with that of unconditional beamforming, where each base station beamforms to its own users, irrespective of the number of antennas N_t at the base stations. With unconditional beamforming, the typical mobile user is subject to interference from all the other base stations in the network, and the interference power is a shot noise process from all the interferers.

Figure 2 plots the probability of coverage versus the SINR threshold T for increasing $d_{N_t} = N_t - N$ at the transmitters, and for fixed average cluster size $\lambda_b/\lambda_c = 3$. The probability of coverage increases with increasing d_{N_t} , $d_{N_t} = 3, d_{N_t} = 7$. For low SINR, and for moderate SNR single-cell beamforming outperforms ICIN for $d_{N_t} = 3$. ICIN outperforms beamforming as the SINR threshold increases. This can be justified by the tradeoff between the decrease in the signal power for ICIN with the decrease in the interference power at low SINR. At higher SINR values, the system is more interference limited, and decreasing the interference when using ICIN outperforms boosting the signal power when using

$$\text{SINR}_{\text{nic}, N_t} = \frac{\gamma_0 \|\mathbf{h}_0\|^2}{\sum_{\mathbf{b}_\ell \in \Pi_b/V^{(c)}(\mathbf{b}_0)} \gamma_{0,\ell} |\mathbf{g}_{0,\ell}^* \mathbf{f}_\ell|^2 + \sum_{\mathbf{b}_\ell \in V^{(c)}(\mathbf{b}_0)} \gamma_{0,\ell} |\mathbf{g}_{0,\ell}^* \mathbf{f}_\ell|^2 + \sigma^2} = \frac{(1+r_0)^{-\alpha} \|\mathbf{h}_0\|^2}{I_{\text{out}} + I_{\text{in}} + \frac{1}{\text{SNR}}}, \quad (28)$$

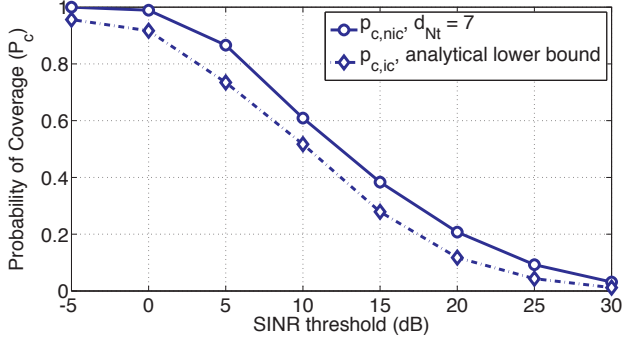


Fig. 3. The probability of coverage for increasing SINR threshold. $p_{c,ic}$ obtained by simulations is compared to the analytical lower bound derived in Result 1. The average number of base stations in the cell is 3 and the pathloss exponent is 4.

beamforming. Moreover, for ICIN, as the clustering is done at random, when the base station is at the edge of the cluster, the interference from adjacent clusters remains dominant, leading to a smaller decrease in the interference power and hence lower ICIN coverage gains. For $d_{N_t} = 3$, ICIN outperforms no nulling in coverage starting at $T = 7$ dB. This threshold decreases with increasing d_{N_t} . For $d_{N_t} = 7$, ICIN outperforms no nulling for all the T values of interest. Figure 2 also plots the coverage probability performance for fixed lattice grid clustering proposed in [19], for $d_{N_t} = 7$. We can conclude from the comparison that the two models are equivalent in terms of coverage performance.

Figure 3 compares the probability of coverage obtained from Monte Carlo simulations with the bound derived in Result 1 for $d_{N_t} = 7$ and average cluster size equal to 3. Figure 3 shows that the lower bound on the probability of coverage exhibits the same behavior as the Monte Carlo simulation. It is sufficiently accurate, to within 0.1 in probability, and can provide insights on the performance of the clustered coordination system.

Figure 4 plots the average rate obtained with ICIN as a function of average cluster size, for $d_{N_t} = 4$. It compares the average rate with equal bit allocation limited feedback (LF-EBA) with and without bias for the desired channel, and the average rate with adaptive limited feedback. The average rate with no interference nulling is also shown for comparison. For a fixed feedback budget at each receiver of $B_{\text{tot}} = 50$, Figure 4 shows that as the average cluster size increases, the average rate with ICIN increases. This is due to the decrease in the interference terms as more and more base stations are added to the cluster. The same holds for the beamforming strategy, as the increase in the number of antennas at each base station as a function of the cluster size increases the signal term, leading to an increase in SINR. For adaptive limited feedback, the average rate increases with the average cluster size, similarly to the increase of ICIN with perfect CSI. ICIN with adaptive limited feedback outperforms no

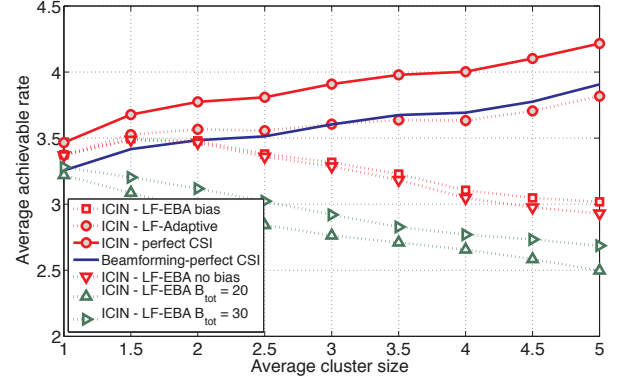


Fig. 4. The average rate as a function of average cluster size, for $N_t = N+4$. τ (with no ICIN) also shown for comparison. The feedback budget per mobile user is fixed $B_{\text{tot}} = 50$ for all the curves except the LF-EBA curves with $B_{\text{tot}} = \{20, 30\}$ indicated in the legend. The performance of beamforming (no ICIN) with limited feedback is almost equivalent to the performance with perfect CSI. LF-EBA-Bias denotes the equal bit allocation scheme with extra bits resulting from rounding to an integer bit value given to the desired user. LF-EBA-no Bias denotes the equal bit allocation scheme with the extra bits not used.

ICIN for moderate average cluster sizes up to $\lambda_b/\lambda_c = 4$. It performs almost similarly to no ICIN for larger cluster sizes. For limited feedback beamforming with equal bit partitioning however, the average rate increases, reaches a maximum at $\lambda_b/\lambda_c = 2$, then decreases. This is justified by the double increase in quantization error due to the decrease in the number of bits per channel and decrease in the number of bits per antenna. Limited feedback with equal bit partitioning and biasing towards the desired channel, through allocating the extra bits available after rounding the bit allocations to integer values, as discussed in Section V, performs better than limited feedback with equal bit partitioning and no desired channel biasing. The extra bits available at the mobile station from the remainder of the division of B_{tot} by $N+1$ are more judiciously used to quantize the desired signal in the equal bit allocation with bias. To further illustrate the tradeoff of the average rate with equal bit partitioning with the average cluster size, we plot the average rate performance of LF-EBA with biasing for $B_{\text{tot}} = \{20, 30\}$ in the same figure. For low feedback budget, the maximum is achieved at an average cluster size of 1.

Figure 5 plots the mean loss in rate versus the total number of bits B_{tot} available at the receiver for $\lambda_b/\lambda_c = 3$, and $d_{N_t} = 5$. The figure also shows the analytical upper bound derived in Result 3 for comparison. The bound is sufficiently tight for all values of B_{tot} . The gap is due to the bounds on the quantization errors in the RVQ analysis as well as the Jensen's inequality and the Gamma second order moment matching. Limited feedback with adaptive bit allocation is shown to significantly decrease the mean loss in rate, as compared to equal bit allocation. To show the decrease of the mean loss in rate for adaptive limited feedback for large values of B_{tot} , we

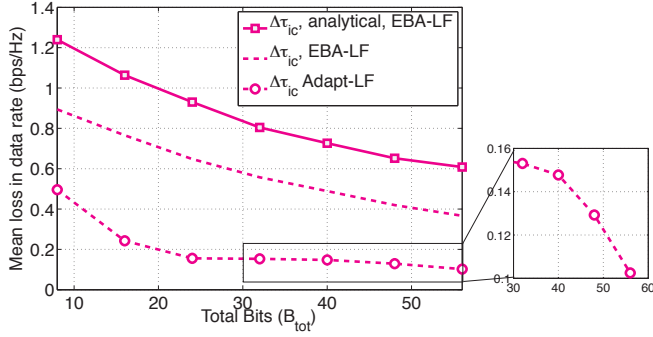


Fig. 5. The mean loss in rate versus the feedback budget per mobile B_{tot} is shown. $N_t - N = 5$, and average cluster size is fixed at $\lambda_b/\lambda_c = 3$.

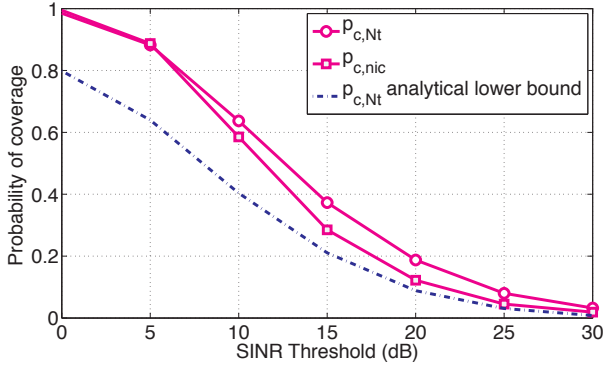


Fig. 6. The probability of coverage for increasing SINR threshold. p_{c,ic,N_t} obtained by simulations is compared to the analytical lower bound derived in Result 1. The average number of base stations in the cell is 3 and the pathloss exponent is 4.

zoom in on $B_{\text{tot}} > 30$. The mean loss in rate with adaptive limited feedback decreases as the number of bits increase, albeit at a lower rate than that with equal bit partitioning.

Figure 6 compares the probability of coverage obtained from Monte Carlo Simulations with the bound derived in Section VI, for $N_t = 10$ and average cluster size equal to 3. The Figure shows that the lower bound on the probability of coverage exhibits the same behavior as the Monte Carlo simulation. The bound, however is loose for small SINR threshold values. This is due to using the circumscribed and inscribed circle to bound the interference power for coordination and no coordination.

Figure 7 plots the average rate obtained with ICIN using the thresholding policy in Section VI, as a function of average cluster size, for increasing number of antennas $N_t = \{6, 8, 12\}$. The achievable rate with unconditional beamforming τ_{nic,N_t} is also shown for comparison. τ_{nic,N_t} does not depend on the average cluster size; it is thus almost constant for all values of λ_b/λ_c . τ_{ic,N_t} increases with increasing λ_b/λ_c , reaches a maximum, then decreases towards τ_{nic,N_t} . This is due to the thresholding policy where the feasibility of ICIN depends on the number of interferers per cluster. When λ_b/λ_c is large compared to the number of antennas, ICIN feasibility decreases, and hence single-user beamforming becomes more prevalent. The gains from coordination depend on the number of antennas at the base stations and the average cluster size. For $N_t = 12$ for example, as the average cluster size increases,

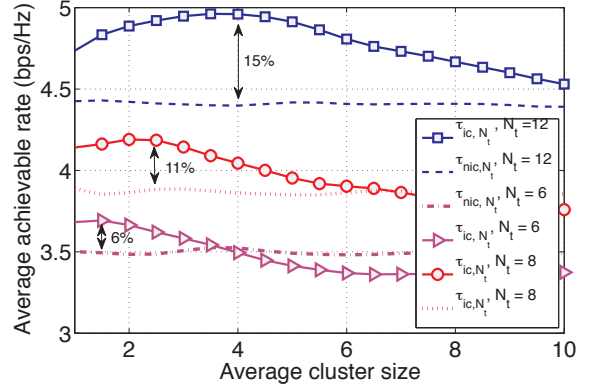


Fig. 7. The average rate τ as a function of the average cluster size, for increasing $N_t = \{6, 8, 12\}$. τ (no ICIN) is also shown for comparison. τ_{ic,N_t} increases with λ_b/λ_c , reaches a maximum and then decreases. The gains from ICIN depend on the number of antennas N_t at the base stations.

the average rate increases, reaches a maximum at around $\lambda_b/\lambda_c = 4$ and then decreases, until it reaches τ_{nic,N_t} . As the number of antennas increases, ICIN feasibility increases, and the average cluster size where ICIN with thresholding attains maximum gains increases. The maximum of τ_{ic,N_t} depends on the average cluster size, the number of antennas N_t and the variance of the cluster size. The variance of the cluster size is a function of the densities λ_b and λ_c . As N_t increases, τ_{ic,N_t} increases, and the relative gain from interference coordination increases. It reaches 15% for $N_t = 12$ and 8% for $N_t = 6$.

VIII. CONCLUSION

In this paper, we analyzed intra-cluster interference coordination for randomly deployed base stations. To cluster the randomly deployed base stations, we proposed a random clustering strategy that overlays an independent Poisson point process on the base stations point process. We assumed that the base stations connected to the closest cluster center form a cluster. We showed that the average cluster size can be optimized with respect to the number of antennas at the base stations to provide the maximum gains from ICIN. We further analyzed the performance of per cluster ICIN with limited feedback CSI. We showed that limited feedback CSI hinders the gains of coordination, and results in significant loss in rate, when equal bit allocation is used. Adaptive bit allocation, optimized as a function of the signal strengths, recover the gains of clustered coordination. One takeaway from this paper is that analysis of cooperative multi-cell systems, for randomly deployed base stations, is possible using hierarchical association. Ongoing work includes using the same setup to analyze the performance of clustered coordination with CSI and user data sharing. It also includes deriving an analytical framework for dynamic user-driven clustering, using the same framework.

APPENDIX A PROOF OF LEMMA 1

Conditioned on b_0 being at a distance r_0 from u_0 , the interference outside a ball of radius $r_m - r_0 - r_1$ away from

u_0 , the probability of coverage is given by

$$p_{c,ic} = \mathbb{E}_{r_m, r_0, r_1} \left\{ \mathbb{P} \left[|\mathbf{h}_0^* \mathbf{f}_0|^2 \geq \frac{T}{(1+r_0)^{-\alpha}} \left(I_{B(u_0)} + \frac{1}{\text{SNR}} \right) \middle| r_0, r_m, r_1 \right] \right\} \\ \stackrel{(a)}{=} \int_0^\infty f_{r_1}(r_1) \int_0^\infty f_{r_0}(r_0) \int_{r_0}^\infty f_{r_m}(r_m) \int_{-\infty}^\infty e^{-\frac{2j\pi s L(r_0)T}{\text{SNR}}} \\ \mathcal{L}_{I_{r_m}}(2j\pi \ell(r_0)Ts) \frac{\left(\frac{1}{-2j\pi s + 1} \right)^{N_t - N} - 1}{2j\pi s} ds dr_m dr_0 dr_1.$$

(a) is derived using the expression in [36] for the probability of coverage using general fading distributions. This expression is applicable here since the desired signal power $|\mathbf{h}_0^* \mathbf{f}_0|^2$ has a finite first moment and admits a square integrable density. The interference I_{r_m} is square integrable using the path-loss model $(1+r)^\alpha$ reminiscent of the pathloss model $(1+Ar)^\alpha$ in [23]. The distribution of r_1 is given by $f_r(r_1) = 2\pi\lambda_c r_1 e^{-\pi r_1^2 \lambda_c}$.

The aggregate interference considered outside a ball of radius $r_m - r_0 - r_1$ results in an upper bound on the aggregate interference due to the fact that less area is excluded from the calculations. The inter-cluster interference can also be bounded by the interference outside a ball of radius r_m centered at u_0 , corresponding to a slightly larger area to be excluded from the calculations than $r_m - r_0 - r_1$. This averaged over the spatial realizations, results in a good lower bound on the probability of coverage as illustrated in Section VII. The lower bound is finally given by the expression in Lemma 1.

APPENDIX B PROOF OF REMARK 1

The PMF of N is computed as the Poisson distributed number of base stations inside a cluster of size t , such that this cluster contains one base station chosen at random from the process Π_b .

To derive the distribution of the size t of the cluster conditioned on the availability of one base station chosen at random inside the cluster cell, we first need an expression for the distribution of the unconditioned size x of a Voronoi cluster. As there is no exact result known for the size distribution of the Poisson-Voronoi cell, we make use of a two-parameter Gamma function fit of the distribution of the normalized cell size, derived in [29],

$$f_X(x) = \frac{3.5^{3.5}}{\Gamma[3.5]} x^{2.5} \exp(-3.5x). \quad (30)$$

Let I be the indicator that a base station chosen at random is located inside a cluster cell. The PDF of the size conditioned on $I = 1$ is derived from $f_X(x)$

$$f_{X|I=1}(t) = \frac{f_{X,I=1}(t)}{\mathbb{P}[I=1]} = \frac{\mathbb{P}[I=1|X=t]f_X(t)}{\mathbb{P}[I=1]} \\ \stackrel{(a)}{=} ct f_X(t) = \frac{3.5^{4.5}}{\Gamma[4.5]} t^{3.5} \exp(-3.5t), \quad (31)$$

where c is a constant such that $\int_0^\infty f_{X|I=1}(t)dt = 1$, and (a) is derived knowing that a randomly chosen base station in Π_b is uniformly distributed in the plane of interest and its probability of being inside an area with a given size is proportional to that

size. The PMF of the number of interferers N inside a cluster cell containing one randomly chosen base station is thus

$$p_N(n) = \int_0^\infty \mathbb{P}[N=n|t] f_{X|I=1}(t) dt \\ \stackrel{(a)}{=} \int_0^\infty \frac{(\lambda_b t)^n e^{-\lambda_b t}}{(n)!} \frac{3.5^{4.5}}{\Gamma[4.5]} t^{3.5} \exp(-3.5t) dt \\ = \frac{3.5^{4.5} \Gamma(n+4.5) (\lambda_b/\lambda_c)^n}{\Gamma(4.5) n! (\lambda_b/\lambda_c + 3.5)^{n+4.5}}. \quad (32)$$

APPENDIX C PROOF OF RESULT 3

For equal-bit-allocation, the expected residual interference is bounded as

$$\mathbb{E} \left\{ \sum_{\ell=1}^N (1+r_{0,\ell})^{-\alpha} \Gamma \left(\frac{2N_t-1}{N_t-1} \right) 2^{-\lfloor \frac{B_{\text{tot}}}{N+1} \rfloor \frac{1}{N_t-1}} \right\} \\ = \mathbb{E} \left\{ N_t \Gamma \left(\frac{2N_t-1}{N_t-1} \right) 2^{-\lfloor \frac{B_{\text{tot}}}{N+1} \rfloor \frac{1}{N_t-1}} \sum_{\ell=1}^N (1+r_{0,\ell})^{-\alpha} \right\} \\ \stackrel{(a)}{\leq} \mathbb{E} \left\{ \Gamma \left(\frac{2N_t-1}{N_t-1} \right) 2^{-\lfloor \frac{B_{\text{tot}}}{N+1} \rfloor \frac{1}{N_t-1}} N \mathbb{E} \left\{ (1+r_{0,1})^{-\alpha} \right\} \right\} \\ \stackrel{(b)}{=} \sum_{n=0}^\infty \left\{ \Gamma \left(\frac{2N_t-1}{N_t-1} \right) n 2^{-\lfloor \frac{B_{\text{tot}}}{n+1} \rfloor \frac{1}{N_t-1}} P_N(n) \right\} \mathbb{E} \left\{ (1+r_{0,1})^{-\alpha} \right\}, \quad (33)$$

where (a) follows by upper bounding the sum of path-loss functions from the interfering cells inside each cluster cell by the path-loss function from the closest interfering base station, $r_{0,1}$. Because the distances $r_{0,\ell}^2$ are 1-D PPP with intensity $\pi\lambda_b$, the random variable $\pi\lambda_b r_{0,1}^2$ has an exponential distribution with parameter 1, $r_{0,1}$ thus has a Rayleigh fading distribution $r_{0,1} \sim \text{Rayleigh}(1/\sqrt{2\pi\lambda_b})$. Therefore

$$\mathbb{E} \left\{ (1+r_{0,1})^{-\alpha} \right\} = \int_0^\infty \int_0^\infty (1+x)^{-\alpha} \frac{x}{2\pi\lambda_b} e^{-\frac{x^2}{4\pi\lambda_b}} f_{r_0}(r_0) dx dr_0.$$

(b) follows from expressing the expectation with respect to N by its definition as a function of the PMF of N , $P_N(n)$.

To compute $\mathbb{E} \left\{ \log_2(\sigma^2 + I_{\text{out}}) \right\}$, we invoke the Gamma approximation of I_{out} . The $\Gamma(k, \theta)$ random variable with the same mean and variance as I_{out} with $|\mathbf{g}_{0,\ell}^* \mathbf{f}_\ell|^2 \sim \exp(1)$ has the parameters k and θ given by $k = \frac{(\mathbb{E}\{I_{\text{out}}\})^2}{\text{var}(x)}$ and $\theta = \frac{\text{var}(x)}{\mathbb{E}\{I_{\text{out}}\}}$, respectively. The expected value of $I_{\text{out}} = k\theta$; the logarithm of the interference $I_{\text{out}} = \Gamma(k, \theta)$, with a high interference-to-noise ratio (INR) approximation is given by

$$\mathbb{E} \left\{ \log_2(I_{\text{out}}) \right\} = \log_e(2) \psi(k) + \log_2(\theta). \quad (34)$$

where $\psi(k)$ is the digamma function.

APPENDIX D PROOF OF RESULT 4

We consider the terms in the mean loss in rate that correspond to B_0 . Per spatial realization, given N and $r_{0,\ell}$, the objective function reduces to

$$\log_2(e) \Gamma\left(\frac{N_t}{N_t-1}\right) 2^{-\frac{B_0}{N_t-1}} + \log_2(e) \frac{\Gamma\left(\frac{2N_t-1}{N_t-1}\right)}{\mathbb{E}\{I_{out}\}+1/\text{SNR}} |\mathcal{K}| 2^{-\frac{B_{tot}-B_0}{|\mathcal{K}|(N_t-1)}} \prod_{\ell \in \mathcal{K}} (1+r_{0,\ell})^{-\frac{\alpha}{|\mathcal{K}|}}. \quad (35)$$

We rewrite the objective function as

$$\begin{aligned} & 2^{-\frac{B_0}{N_t-1}} + \frac{\Gamma\left(\frac{2N_t-1}{N_t-1}\right)}{\mathbb{E}\{I_{out}\}+1/\text{SNR}} \frac{|\mathcal{K}| 2^{-\frac{B_{tot}-B_0}{|\mathcal{K}|(N_t-1)}} \prod_{\ell \in \mathcal{K}} (r_{0,\ell})^{-\frac{\alpha}{|\mathcal{K}|}}}{\Gamma\left(\frac{N_t}{N_t-1}\right)} 2^{\frac{B_0}{|\mathcal{K}|(N_t-1)}} \\ & = 2^{-\frac{B_0}{N_t-1}} + C_0 2^{\frac{B_0}{|\mathcal{K}|(N_t-1)}}, \end{aligned} \quad (36)$$

and we invoke the arithmetic mean-geometric mean inequality

$$2^{-\frac{B_0}{N_t-1}} + C_0 2^{\frac{B_0}{|\mathcal{K}|(N_t-1)}} \leq 2\sqrt{2^{-\frac{B_0}{N_t-1}} C_0 2^{\frac{B_0}{|\mathcal{K}|(N_t-1)}}}$$

to find the minimum of the objective function. We solve for B_0 that satisfies the equality $2^{-\frac{B_0}{N_t-1}} = C_0 2^{\frac{B_0}{|\mathcal{K}|(N_t-1)}}$,

$$B_0 = -(N_t - 1) \log_2(C_0) \frac{|\mathcal{K}|}{|\mathcal{K}| + 1}.$$

Replacing C_0 by its value from (36) yields the result for the low SNR approximation.

REFERENCES

- [1] D. Gesbert, S. Hanly, H. Huang, S. Shamai, O. Simeone, and W. Yu, "Multi-cell MIMO cooperative networks: A new look at interference," *IEEE J. Select. Areas Commun.*, vol. 28, no. 9, pp. 1380–1408, Dec. 2010.
- [2] A. Papadogiannis, D. Gesbert, and E. Hardouin, "A dynamic clustering approach in wireless networks with multi-cell cooperative processing," in *Proc. of IEEE Int. Conf. on Commun.*, May 2008, pp. 4033–4037.
- [3] A. Lozano, J. G. Andrews, and R. W. Heath Jr, "On the limitations of cooperation in wireless networks," in *Proc. of Information Theory and Application Workshop (ITA)*, Feb. 2012.
- [4] O. Simeone, O. Somekh, H. Poor, and S. Shamai, "Local base station cooperation via finite-capacity links for the uplink of wireless networks," *IEEE Trans. Inform. Theory*, vol. 55, no. 1, pp. 190–204, Jan. 2009.
- [5] J. Zhang, R. Chen, J. G. Andrews, A. Ghosh, and R. W. Heath Jr, "Networked MIMO with clustered linear precoding," *IEEE Trans. Wireless Commun.*, vol. 8, no. 4, pp. 1910–1921, Apr. 2009.
- [6] A. Barbieri, P. Gaal, T. J. Geirhofer, D. Malladi, Y. Wei, and F. Xue, "Coordinated downlink multi-point communications in heterogeneous cellular networks," in *Proc. of the Workshop on Information Theory and Its Applications*, 2012.
- [7] S. Shamai and B. M. Zaidel, "Enhancing the cellular downlink capacity via co-processing at the transmitting end," in *Proc. of IEEE Veh. Technol. Conf. - Spring*, vol. 3, May 6–9, 2001, pp. 1745–1749.
- [8] J. Ekbal and J. M. Cioffio, "Distributed transmit beamforming in cellular networks - a convex optimization perspective," in *Proc. of IEEE Int. Conf. on Commun.*, vol. 4, 2005, pp. 2690–2694.
- [9] E. Jorwiesk, E. G. Larsson, and D. Danev, "Complete characterization of the pareto boundary for the MISO interference channel," *IEEE Trans. Signal Processing*, vol. 56, no. 10, pp. 5292–5296, Oct. 2008.
- [10] B. L. Ng, J. S. Evans, S. V. Hanly, and D. Aktas, "Distributed downlink beamforming with cooperative base stations," *IEEE Trans. Inform. Theory*, vol. 54, no. 12, pp. 5491–5499, Dec. 2008.
- [11] C. K. Ng and H. Huang, "Linear precoding in cooperative MIMO cellular networks with limited coordination clusters," *IEEE J. Select. Areas Commun.*, vol. 28, no. 9, pp. 1446 – 1454, Dec. 2010.
- [12] J. Zhang and J. G. Andrews, "Adaptive spatial intercell interference cancellation in multicell wireless networks," *IEEE J. Select. Areas Commun.*, vol. 28, no. 9, pp. 1455 – 1468, Dec. 2010.
- [13] R. Bhagavatula and R. Heath Jr, "Adaptive bit partitioning for multicell intercell interference nulling with delayed limited feedback," *IEEE Trans. Signal Processing*, vol. 59, no. 8, pp. 3824–3836, Aug. 2011.
- [14] S. Kaviani, O. Simeone, W. Krzymien, and S. Shamai, "Linear precoding and equalization for network MIMO with partial coordination," *IEEE Trans. Veh. Technol.*, vol. PP, no. 99, pp. 1–1, Feb. 2012.
- [15] G. Foschini, K. Karakayali, and R. Valenzuela, "Coordinating multiple antenna cellular networks to achieve enormous spectral efficiency," *IEEE Proc. Comm.*, vol. 153, pp. 548–555, Aug. 2006.
- [16] J. G. Andrews, F. Baccelli, and R. Krishna Ganti, "A tractable approach to coverage and rate in cellular networks," *IEEE Transactions on Communications*, vol. 59, no. 11, pp. 3122–3134, Nov. 2011.
- [17] P. Marsch and G. Fettweis, Eds., *Coordinated Multi-Point in Mobile Communications. From Theory to Practice*, 1st ed. Cambridge University Press, 2011.
- [18] F. Baccelli, M. Klein, M. Lebourges, and S. Zuyev, "Stochastic geometry and architecture of communication networks," *Journal of Telecommunications Systems*, vol. 7, no. 1, pp. 209–227, 1997.
- [19] K. Huang and J. G. Andrews, "A closer look at multi-cell cooperation via stochastic geometry and large deviations," *submitted to IEEE Trans. Inform. Theory*, Apr. 2012. [Online]. Available: <http://arxiv.org/abs/1204.3167>
- [20] D. J. Love, R. W. Heath, Jr., V. K. N. Lau, D. Gesbert, B. Rao, and M. Andrews, "An overview of limited feedback in wireless communication systems," *IEEE J. Select. Areas Commun.*, vol. 26, no. 8, pp. 1341–1365, Oct. 2008.
- [21] S. Akoum, M. Kountouris, and R. W. Heath Jr, "On imperfect CSI for the downlink of a two-tier network," in *Proc. of IEEE Intl. Symp. on Info. Theory*, Jul. 2011, pp. 553–557.
- [22] B. Ozbek and D. Le Ruyet, "Adaptive limited feedback for intercell interference cancellation in cooperative downlink multicell networks," in *Proc. of Intl. Symp. on Wireless Comm. Systems*, Sept. 2010, pp. 81–85.
- [23] F. Baccelli and B. Błaszczyszyn, *Stochastic geometry and wireless networks. Volume I: theory*. NOW publishers, 2009.
- [24] S. Weber and J. G. Andrews, *Transmission Capacity of Wireless Networks*, Foundations and T. in Networking, Eds. NOW Publishers, Feb. 2012.
- [25] N. Jindal, J. G. Andrews, and S. Weber, "Multi-antenna communication in ad hoc networks: achieving MIMO gains with SIMO transmission," *IEEE Trans. Commun.*, vol. 59, pp. 529–540, Feb. 2011.
- [26] S. Akoum, M. Kountouris, M. Debbah, and R. Heath Jr, "Spatial interference mitigation for multiple input multiple output ad hoc networks: MISO gains," in *Proc. of IEEE Asilomar Conf. on Signals, Systems, and Computers*, Nov. 2011.
- [27] M. Sharif and B. Hassibi, "On the capacity of MIMO broadcast channels with partial side information," *IEEE Trans. Inform. Theory*, vol. 51, no. 2, pp. 506–522, 2005.
- [28] R. Bhagavatula, R. Heath Jr, and B. Rao, "Limited feedback with joint CSI quantization for multicell cooperative generalized eigen vector beamforming," in *Proc. of IEEE Intl. Conf. on Acoustics Speech and Signal Proc.*, Mar. 2010.
- [29] J.-S. Ferenc and Z. Neda, "On the size distribution of Poisson Voronoi cells," *Physica A*, vol. 385, pp. 518–526, 2007.
- [30] S. G. Foss and S. A. Zuyev, "On a Voronoi aggregative process related to a bivariate poisson process," *Adv. Appl. Prob.*, vol. 28, pp. 965–981, 1996.
- [31] N. Jindal, "MIMO broadcast channels with finite rate feedback," *IEEE Trans. Inform. Theory*, vol. 52, no. 11, pp. 5045–5060, Nov. 2006.
- [32] G. Caire, N. Jindal, M. Kobayashi, and N. Ravindran, "Multiuser MIMO achievable rates with downlink training and channel state feedback," *IEEE Transactions on Information Theory*, vol. 56, no. 6, pp. 2845–2866, Jun. 2010.
- [33] R. W. Heath Jr., T. Wu, and Y. H. Kwon, "Multi-user MIMO in distributed antenna systems with out-of-cell interference," *IEEE Trans. Signal Processing*, vol. 59, no. 10, pp. 4885–4899, Oct. 2011.
- [34] D. Stoyan, W. Kendall, and J. Mecke, *Stochastic Geometry and Its Applications*. John Wiley and Sons, Ltd., 1995.
- [35] P. Calka, "The distributions of the smallest disks containing the Poisson-Voronoi typical cell and the Crofton cell in the plane," *Advances in Applied Probability*, vol. 34, no. 4, pp. 702–717, Dec. 2002.
- [36] F. Baccelli, B. Błaszczyszyn, and P. Muhlethaler, "Stochastic analysis of spatial and opportunistic Aloha," *IEEE J. Select. Areas Commun.*, vol. 27, no. 7, pp. 1105–1119, sept. 2009.